HHS Public Access

Author manuscript

Neuroscience. Author manuscript; available in PMC 2018 December 05.

Published in final edited form as:

Neuroscience. 2018 September 15; 388: 128–138. doi:10.1016/j.neuroscience.2018.07.012.

Subregion-Specific Impacts of Genetic Loss of Diazepam Binding Inhibitor on Synaptic Inhibition in the Murine Hippocampus

Connor D. Courtney[a] and **Catherine A. Christian**[a,b,c,*]

[a]Neuroscience Program, University of Illinois at Urbana-Champaign, Urbana, IL, United States

[b]Department of Molecular and Integrative Physiology, University of Illinois at Urbana-Champaign, Urbana, IL, United States

[c]Beckman Institute for Advanced Science and Technology, University of Illinois at Urbana-Champaign, Urbana, IL, United States

Abstract

Benzodiazepines are commonly prescribed to treat neurological conditions including epilepsy, insomnia, and anxiety. The discovery of benzodiazepine-specific binding sites on γ-aminobutyric acid type-A receptors ($GABA_ARs$) led to the hypothesis that the brain may produce endogenous benzodiazepine-binding site ligands. An endogenous peptide, diazepam binding inhibitor (DBI), which can bind these sites, is thought to be capable of both enhancing and attenuating GABAergic transmission in different brain regions. However, the role that DBI plays in modulating $GABA_ARs$ in the hippocampus remains unclear. Here, we investigated the role of DBI in modulating synaptic inhibition in the hippocampus using a constitutive DBI knockout mouse. Miniature and evoked inhibitory postsynaptic currents (mIPSCs, eIPSCs) were recorded from CA1 pyramidal cells and dentate gyrus (DG) granule cells. Loss of DBI signaling increased mIPSC frequency and amplitude in CA1 pyramidal cells from DBI knockout mice compared to wild-types. In DG granule cells, conversely, the loss of DBI decreased mIPSC amplitude and increased mIPSC decay time, indicating bidirectional modulation of $GABA_AR$-mediated transmission in specific subregions of the hippocampus. eIPSC paired-pulse ratios were consistent across genotypes, suggesting that alterations in mIPSC frequency were not due to changes in presynaptic release probability. Furthermore, cells from DBI knockout mice did not display altered responsiveness to pharmacological applications of diazepam, a benzodiazepine, nor flumazenil, a benzodiazepine-binding site antagonist. These results provide evidence that genetic loss of DBI alters synaptic inhibition in the adult hippocampus, and that the direction of DBI-mediated modulation can vary discretely between specific subregions of the same brain structure.

Keywords

GABA; benzodiazepine; electrophysiology; diazepam; flumazenil; paired-pulse ratio

*Corresponding author: Catherine A. Christian, University of Illinois at Urbana-Champaign, 506 S. Mathews Ave. 523 Medical Sciences Building, Urbana, IL 61801, USA, cathchri@illinois.edu, Telephone: (217) 244-8230, Fax: (217) 244-5858.

Introduction

Benzodiazepines (BZs) are among the most commonly prescribed medications and are used to treat a variety of disorders including anxiety, insomnia, muscle spasms, and epilepsy. BZs bind to specific sites located at the interface between α and γ subunits of type-A receptors for the neurotransmitter γ-aminobutyric acid ($GABA_A$Rs) (Braestrup and Squires, 1977; Möhler and Okada, 1977; Sieghart, 2015). When bound, BZs typically promote the enhancement of synaptic inhibition by increasing GABA affinity and the frequency of channel opening, thus potentiating inhibitory postsynaptic currents (IPSCs) (Twyman et al., 1989; Bianchi, 2010). The discovery of BZ-specific binding sites on $GABA_A$Rs fueled the hypothesis that the brain may produce endogenous BZ-binding site ligands (Iversen, 1977; Costa and Guidotti, 1985). Despite decades of research, however, only modest advancements were made in the search for these “endozepines” (Farzampour et al., 2015).

The presence of endozepines in the brain is supported by *in vitro* studies utilizing the BZ-binding site antagonist flumazenil (FLZ) (Hunkeler, 1981). In the hippocampus, the amplitude of inhibitory postsynaptic potentials in rat CA1 pyramidal cells was reduced after FLZ application (King et al., 1985), suggesting that the blockade of the $GABA_A$R BZ-binding site impeded the potentiation of inhibition by an endogenous ligand. Additionally, FLZ reduced IPSC decay time in the thalamic reticular nucleus (Christian et al., 2013; Christian and Huguenard, 2013) and in cultured cortical neurons (Vicini et al., 1986). Similarly, FLZ reduced the amplitude of electrically evoked inhibitory postsynaptic currents (eIPSCs) in CA1 pyramidal cells following the induction of long-term potentiation (Xu and Sastry, 2005). In dentate gyrus (DG) granule cells, FLZ reduced miniature IPSC (mIPSC) decay time in pilocarpine-treated epileptic rats but not in control rats (Leroy et al., 2004), suggesting putative region-specific effects of endozepines in the hippocampus in both pathological and non-pathological states.

The endogenous peptide diazepam binding inhibitor (DBI) appears to exert endozepine actions. DBI, also known as acyl-CoA binding protein, is a 10 kDa protein initially identified for its ability to displace radiolabeled diazepam from BZ-binding sites on $GABA_A$Rs (Guidotti et al., 1983). Although DBI also has a role as an intracellular signaling molecule critical in fatty acid biosynthesis (Neess et al., 2015), several studies indicate that DBI can be secreted extracellularly in the brain and modulate $GABA_A$R function. DBI protein immunoreactivity is seen in both neurons (Alho et al., 1985; Alho et al., 1989; Christian and Huguenard, 2013) and astrocytes (Alho et al., 1991; Malagon et al., 1993; Vidnyánszky et al., 1994; Christian and Huguenard, 2013) and can be detected in several brain regions, including the hippocampus (Ball et al., 1989; Ferrarese et al., 1989). Multiple DBI cleavage products, including octadecaneuropeptide (ODN), triakontatetraneuropeptide, and octapeptide (Ferrero et al., 1986), are biologically active and capable of displacing BZs from the BZ binding site. However, the precise physiological roles that DBI and its processing products play in the modulation of GABAergic neurotransmission are largely undefined.

The extent to which DBI is capable of modulating $GABA_A$Rs remains controversial, as DBI-dependent modulation of inhibition appears to be specifically localized to certain brain

regions, and both agonistic and inverse agonistic actions have been reported. Exogenous application of DBI reduced IPSC amplitude in cultured spinal neurons, and this effect was reversed after FLZ application (Bormann, 1991), suggesting negative allosteric modulation of $GABA_A$Rs at the BZ-binding site. Similarly, inverse agonistic actions were demonstrated in the subventricular zone, in which ODN, a DBI fragment, enhanced neurogenesis via negative allosteric modulation of $GABA_A$R-mediated currents (Alfonso et al., 2012). The negative allosteric modulatory role of DBI as a critical component in neurogenesis was further demonstrated in the hippocampal subgranular zone, in which DBI-dependent attenuation of $GABA_A$R currents promoted stem cell proliferation (Dumitru et al., 2017). By contrast, we recently demonstrated that DBI acts as a positive allosteric modulator of $GABA_A$Rs in the thalamic reticular nucleus (Christian et al., 2013). $GABA_A$R potentiation in this region was absent in mice genetically lacking DBI signaling, and this effect was rescued after viral reintroduction of DBI. DBI endozepine effects were not seen in the neighboring ventrobasal nucleus of the thalamus, providing further evidence that DBI modulatory effects may be subregion-specific within larger brain structures. In summary, it appears that DBI is capable of both enhancing and attenuating inhibitory neurotransmission in the brain, and that DBI-dependent modulation of GABAergic inhibition likely varies across different brain areas. Whether DBI is capable of modulating synaptic inhibition in the hippocampus has not been investigated, despite evidence of a role for DBI in modulating hippocampus-dependent behaviors (Liu et al., 2005; Siiskonen et al., 2007; Sherrin et al., 2009).

The purpose of this study was to determine the effects of genetic loss of DBI signaling on synaptic inhibition in the murine hippocampus. We hypothesized that a lack of DBI signaling would lead to altered inhibitory neurotransmission in the hippocampus, and tested this hypothesis using whole-cell patch clamp electrophysiology and pharmacology. Our findings demonstrate that genetic loss of DBI alters GABAergic neurotransmission in the adult hippocampus in a subregion-specific manner.

Experimental Procedures

Animals

The Institutional Animal Care and Use Committee of the University of Illinois at Urbana-Champaign approved all animal procedures. DBI heterozygous ($DBI^{+/-}$) knockout founder mice on the C57BL/6BomTac background strain were obtained from Dr. Susanne Mandrup (University of Southern Denmark). The production of these mice by the Mandrup laboratory was described previously (Neess et al., 2011). At the University of Illinois, the colony was re-derived and backcrossed to the C57BL/6J background (Ujjainwala et al., 2018). Breeding pairs consisted of $DBI^{+/-}$ females crossed with $DBI^{+/-}$ males, yielding $DBI^{+/+}$, $DBI^{+/-}$, and $DBI^{-/-}$ pups (Neess et al., 2011). Mice were bred and housed on a 14:10 h light:dark cycle with food and water available *ad libitum*. Electrophysiology experiments were performed using both male and female $DBI^{+/+}$ and $DBI^{-/-}$ mice 53 to 167 days old.

Brain Slice Preparation

Mice were deeply anesthetized via intraperitoneal (i.p.) injection of pentobarbital (55 mg/kg) and euthanized by decapitation. Brains were immediately dissected and placed in an oxygenated (95% O_2/5% CO_2) ice-cold sucrose slicing solution containing 234 mM sucrose, 11 mM glucose, 2.5 mM KC1, 1.25 mM NaH_2PO_4, 10 mM $MgSO_4$, 0.5 mM $CaC1_2$, and 26 mM $NaHCO_3$. Acute coronal hippocampal slices 300 μm in thickness were prepared using a VT1200S vibratome (Leica Biosystems, Buffalo Grove, IL). Slices were subsequently incubated in oxygenated artificial cerebrospinal fluid (ACSF) containing 2.5 mM KCl, 10 mM glucose, 126 mM NaCl, 1.25 mM NaH_2PO_4. 1 mM $MgSO_4$, 2 mM $CaC1_2$, and 26 mM $NaHCO_3$ at 298 mOsm. Slices were incubated at 32 °C for 1 hour before being transferred to room temperature (21-23 °C) for at least 15 minutes before recording.

Electrophysiology

Slices were transferred to a fully submerged recording chamber on the stage of a BX51WI fixed-staged microscope (Olympus America, Center Valley, PA), and continuously superfused with room-temperature oxygenated ACSF at 2.5 mL/min. Patch-clamp recordings were made using a MultiClamp 700B amplifier, Digidata 1550 digitizer, and Clampex 10.4 software (Molecular Devices, Sunnyvale, CA). For all patch-clamp recordings, pipettes were filled with a near-isotonic CsCl-based intracellular solution containing 135 mM CsCl, 10 mM HEPES, 10 mM EGTA, 2 mM $MgCl_2$, and 5 mM QX-314, pH 7.3 and 290 mOsm. Recording pipettes were created from borosilicate glass using a P-1000 Flaming/Brown micropipette puller (Sutter Instrument, Novato, CA). Pipettes were pulled to have an open-tip resistance of 2-5 MΩ when filled with the internal pipette solution. Individual neurons were visually targeted for recording using differential infrared contrast optics through an sCMOS camera (OrcaFlash 4.0LT, Hamamatsu, Japan).

Whole-cell patch-clamp recordings in both CA1 pyramidal cells and DG granule cells were made in voltage-clamp mode with the membrane potential clamped at −60 mV. Inhibitory postsynaptic currents (IPSCs) were recorded with a 20 kHz sampling rate, low-pass filtered at 4 kHz, and gain set at 10 mV/pA. Series resistance (R_s) was <20 MΩ for all recordings and was not compensated. R_s was monitored every 2-6 minutes by applying 60 5-mV depolarizing steps 20 ms in length from a holding potential of −70 mV, and was calculated by measuring the baseline to the peak of the averaged current responses. Cells with >20% change in R_s during recording were excluded from analyses.

Miniature IPSCs (mIPSCs) were recorded with tetrodotoxin (TTX, 0.5 μM, Abcam, Cambridge, MA) added to the bath solution to limit presynaptic contributions. Evoked IPSCs (eIPSCs) were elicited by electrical stimuli delivered via a bipolar tungsten stimulating electrode (FHC, Bowdoin, ME) placed in either stratum radiatum (CA1) or the DG molecular layer (DG). Stimulus timing and duration was controlled in Clampex and stimulus intensity was controlled using an ISO-Flex stimulus isolator (A.M.P.I., Jerusalem, Israel). For eIPSC experiments, threshold was defined as the intensity at which failures were observed at a rate of approximately 50%, and recordings were made at 1.5x threshold. Paired-pulse ratio (PPR) recordings were made every 20 seconds using a 100-ms inter-stimulus interval between 2 electrical stimuli delivered.

To isolate GABAergic IPSCs, ionotropic glutamate receptors were blocked by either kynurenic acid (1 mM, MilliporeSigma, St. Louis, MO) or a combination of 2-amino-5-phosphonovaleric (APV, 5 μM, Abcam) and 6,7-dinitroquinoxaline-2,3-dione (DNQX, 20 μM, Abcam). Where noted, diazepam (DZP, 1 μM, MilliporeSigma) or flumazenil (FLZ, 1 μM or 5 nM, MilliporeSigma) was added to the bath ACSF solution. Recordings involving DZP/FLZ application were performed by establishing a 6-minute baseline, followed by a 10-minute application of the drug, and a 10-minute washout period.

Data Analysis and Statistics

mIPSCs were analyzed using MiniAnalysis 6.0.7 software (Synaptosoft, Decatur, GA). An event detection threshold was set at 4 pA above baseline. Decay time was calculated as the time for the current to recover from 90% of peak amplitude to 10%. Events that did not recover to baseline before the initiation of a subsequent event or that began during the decay phase of a previous event were excluded from amplitude and decay analyses, but were included in frequency analyses. Evoked IPSCs were analyzed using Clampfit 10.4 (Molecular Devices), and the amplitude of the first response was normalized to peak amplitude to compensate for the variation in eIPSC amplitude across cells. PPR from eIPSCs for each cell was calculated as (mean amplitude of the second response [A2])/(mean amplitude of the first response [A1]) to eliminate the potential of spurious paired-pulse facilitation (Kim and Alger, 2001). Passive electrical properties were calculated using Clampfit 10.4 (Molecular Devices), and no differences were seen between groups in input resistance, series resistance, or cell capacitance.

Data from MiniAnalysis were subsequently transferred to OriginPro 2016 (OriginLab, Northampton, MA) and Excel (Microsoft, Redmond, WA) for statistical analysis. Shapiro-Wilk tests were used to evaluate if data were normally distributed. If data were not normally distributed, log transformations were used to improve normality as noted in the text. For cumulative probability distributions, up to 100 randomly selected mIPSCs per cell were selected so that no individual cells were overrepresented in any group. Probability distribution comparisons were made using two-sample Kolmogorov-Smirnov (KS) goodness-of-fit tests. Group comparisons were made by using either two-way analysis of variance (ANOVA), with sex and genotype as independent variables, or by two-tailed independent (Student's) or paired t-tests. Statistical significance was set at $p<0.05$ for comparisons of means, and at $p<0.001$ for KS tests.

Results

Divergent effects of loss of DBI on mIPSC frequency and amplitude in CA1 and dentate gyrus

To determine if the genetic removal of DBI alters synaptic inhibition in the hippocampus, we used whole-cell patch clamp electrophysiology to record mIPSCs in cells from both $DBI^{+/+}$ and $DBI^{-/-}$ mice of either sex. In CA1 pyramidal cells, two-way ANOVA revealed no significant effect of sex nor a genotype-by-sex interaction in either mIPSC amplitude or frequency ($p>0.05$). Therefore, data from males and females were analyzed together. mIPSC frequency in CA1 pyramidal cells from $DBI^{-/-}$ mice (27 cells from 10 mice) was increased

compared with $DBI^{+/+}$ mice (28 cells from 11 mice) ($p<0.02$, Student's t-test) (Figure 1A-B). Additionally, a modest yet significant increase in mIPSC amplitude was seen in CA1 pyramidal cells from $DBI^{-/-}$ mice (2700 events from 27 cells from 10 mice) compared with $DBI^{+/+}$ mice (2800 events from 28 cells from 11 mice) ($p<0.001$, KS test) (Figure 1C-1D, Table 1). Two-way ANOVA for mIPSC decay time showed a significant effect of sex ($p<0.05$), in which males displayed increased mIPSC decay time compared to females (not shown). However, this effect was seen in both genotypes, and no significant differences in mIPSC decay time were observed between $DBI^{+/+}$ (2800 events from 28 cells from 11 mice) and $DBI^{-/-}$ mice (2700 events from 27 cells from 10 mice) when collapsed across sex (Figure 1E-1F, Table 1). Together, these results reveal that a genetic loss of DBI is capable of modulating GABAergic neurotransmission in adult CA1 pyramidal cells both pre- and postsynaptically.

DBI-mediated effects on inhibition can be specifically localized to distinct subregions of larger brain structures (Christian et al., 2013). To determine if DBI-mediated modulation of hippocampal $GABA_A$Rs is specific to CA1, we also recorded mIPSCs from DG granule cells. Analysis of mIPSC frequency data in DG revealed that the data were not normally distributed. Therefore, a log transformation was used to improve normality. Two-way ANOVA of the transformed data yielded no main effect of sex ($p>0.6$) and no sex-by-genotype interaction ($p>0.05$), so males and females were analyzed together. Additionally, there was no main effect of genotype ($p>0.45$), indicating that mIPSC frequency was not different between $DBI^{+/+}$ and $DBI^{-/-}$ mice in DG granule cells. Indeed, a Student's t-test found no difference in mIPSC frequency between $DBI^{+/+}$ (43 cells from 15 mice) and $DBI^{-/-}$ cells (31 cells from 10 mice) (Figure 2A-2B). Two-way ANOVA of mIPSC amplitude and decay in DG found no main effect of sex ($p>0.35$) and no sex-by-genotype interaction ($p>0.2$) for either parameter, so males and females were analyzed together. In contrast to CA1 pyramidal cells, mIPSC amplitude was decreased in DG granule cells from $DBI^{-/-}$ mice (2929 events from 31 cells from 10 mice) compared to $DBI^{+/+}$ mice (4025 events from 43 cells from 15 mice) ($p<0.001$, KS test) (Figure 2C-2D, Table 1). Furthermore, we found that the loss of DBI increases mIPSC decay time in DG granule cells ($p<0.001$, KS test) (Figure 2E-2F, Table 1). These data further demonstrate that genetic loss of DBI is capable of modulating $GABA_A$Rs in the adult hippocampus, and indicate that DBI-dependent modulation of inhibition is subregion-specific.

Changes in mIPSC frequency are not due to alterations in vesicular release probability

The frequency of miniature postsynaptic currents is typically regarded as a readout of activity-independent presynaptic neurotransmitter release. We thus hypothesized that the changes seen in mIPSC frequency in CA1 pyramidal cells could be due to either alterations in vesicle release probability and/or modifications in synaptic connectivity. To determine if the changes in mIPSC frequency in mice lacking DBI signaling were due to alterations in synaptic vesicle release probability, we investigated the paired-pulse ratio (PPR) of evoked IPSCs in both CA1 pyramidal cells and DG granule cells in $DBI^{+/+}$ and $DBI^{-/-}$ mice. Analysis of PPR is a tool to indirectly measure presynaptic release probability (Dobrunz and Stevens, 1997; Thomson, 2000). A series of two rapidly-induced postsynaptic currents in principal cells of CA1 or DG were evoked using a stimulating electrode placed in either the

stratum radiatum or the DG molecular layer, with an inter-stimulus interval of 100 ms. Two-way ANOVA yielded no effect of sex and no sex-by-genotype interaction in either CA1 or DG, so males and females were analyzed together. In CA1 pyramidal cells, there was no significant difference in the PPR between $DBI^{+/+}$ (8 cells from 7 mice) and $DBI^{-/-}$ mice (8 cells from 5 mice) ($p>0.8$, Student's t-test) (Figure 3A-3E). As expected, we also found no significant difference between $DBI^{+/+}$ mice (17 cells from 8 mice) and $DBI^{-/-}$ mice (18 cells from 8 mice) in the PPR of DG granule cells ($p>0.1$, Student's t-test) (Figure 3C-3D). Furthermore, there were no significant differences between $DBI^{+/+}$ and $DBI^{-/-}$ mice in the coefficient of variation (CV), a measure of response variability (Olmos-Serrano et al., 2010), in either CA1 ($p>0.35$ Student's t-test) or DG ($p>0.1$, Student's t-test) (Figure 3E-3F). Taken together, these results suggest that the release probability of synaptic vesicles in both CA1 and DG is unaltered in mice with a genetic loss of DBI.

Response to DZP and FLZ application is unaltered in $DBT^{-/-}$ mice

DBI binds with high affinity to the BZ binding site on $GABA_A$ receptors (Costa and Guidotti, 1991; Möhler, 2014) and is capable of displacing DZP from the $GABA_AR$ BZ binding site (Guidotti et al., 1983). Therefore, we hypothesized that an absence of DBI signaling would render GABAergic synapses more sensitive to DZP modulation via removal of a competitor at BZ binding sites. CA1 pyramidal cells of both genotypes displayed increases in mIPSC amplitude (Figure 4A-4B) and decay (Figure 4D-4E) in response to DZP compared with baseline control values (all $p<0.01$, paired t-tests). However, no differences between $DBI^{+/+}$ (8 cells from 4 mice) and $DBI^{-/-}$ mice (9 cells from 5 mice) were observed in the strength of the response to DZP; both genotypes exhibited similar increases in mIPSC amplitude ($p>0.7$, Student's t-test) (Figure 4C) and decay time ($p=0.4$ Student's t-test) (Figure 4F). Similar results were seen in DG; granule cells of both genotypes showed increased mIPSC amplitude (Figure 5A-5B) and decay (Figure 5D-5E) with DZP (all $p<0.01$, paired t-tests), but there was no genotype difference in response strength for either parameter ($DBI^{+/+}$: 9 cells from 3 mice; $DBI^{-/-}$: 7 cells from 2 mice) (both $p>0.85$, Student's t-test) (Figure 5C, 5F). No changes in mIPSC frequency with DZP were seen in either genotype (not shown). These results indicate that the genetic loss of DBI signaling does not alter $GABA_AR$ sensitivity to DZP in either CA1 or DG of the hippocampus.

Although we did not observe a difference between genotypes after an application of the BZ-site agonist DZP, we decided to investigate the impacts of the BZ-site antagonist FLZ on synaptic inhibition in $DBI^{+/+}$ and $DBI^{-/-}$ mice. In CA1, no significant differences in mIPSC amplitude were observed between baseline control and after 1 μM FLZ application in cells from either $DBI^{+/+}$ ($p>0.2$, paired t-test) or $DBI^{-/-}$ mice ($p>.1$, paired t-test) (Figure 6A), and there was no genotype difference between $DBI^{+/+}$ and $DBI^{-/-}$ mice in the degree of response to 1 μM FLZ ($p>0.5$, Student's t-test) (Figure 6B). There was also no significant change in mIPSC decay after the application of 1 μM FLZ in CA1 pyramidal cells from either $DBI^{+/+}$ or $DBI^{-/-}$ mice (Figure 6C, paired t-test), and there was no genotype difference in the response to 1 μM FLZ (Figure 6D, Student's t-test). DG granule cells from both $DBI^{+/+}$ and $DBI^{-/-}$ mice, however, exhibited an increase in mIPSC amplitude with 1 μM FLZ (both $p<0.05$, paired t-test) (Figure 7A), although the strength of the response was

not significantly different between $DBI^{+/+}$ and $DBI^{-/-}$ mice ($p>0.25$, Student's t-test) (Figure 7C). No significant change after 1 μM FLZ application was seen in mIPSC decay in DG granule cells from either $DBI^{+/+}$ or $DBI^{-/-}$ mice (both $p>0.1$, paired t-test) (Figure 7D), and the degree of response in DG granule cells was not different between genotypes (Figure 7F, Student's t-test). No changes in mIPSC frequency were seen with 1 μM FLZ in either genotype (not shown).

Although no significant differences were seen in the magnitude of the effect of 1 μM FLZ on mIPSC amplitude between $DBI^{+/+}$ and $DBI^{-/-}$ mice, it is possible that this relatively elevated concentration may have masked a potential endozepine effect. Therefore, we also tested the effects of 5 nM concentration of FLZ in DG granule cells. 5 nM is the EC50 for flumazenil actions on α2-containing $GABA_A$Rs (Ramerstorfer et al., 2010), which are highly expressed in DG granule cells (Sperk et al., 1997). Similarly to 1 μM FLZ, application of 5 nM FLZ increased mIPSC amplitude in DG granule cells from both $DBI^{+/+}$ mice (10 cells from 4 mice) and $DBI^{-/-}$ mice (9 cells from 3 mice) compared to baseline (both $p<0.001$, paired t-test) (Figure 7B). As with the 1 μM concentration, however, no differences were seen between genotypes in the strength of the response ($p=0.3$, Student's t-test) (Figure 7C). Additionally, no differences were seen in mIPSC decay time after 5 nM FLZ application in either $DBI^{+/+}$ or $DBI^{-/-}$ mice (both $p>0.05$) (Figure 7E-F). Together, these data demonstrate that the loss of DBI signaling does not change $GABA_A$R response to FLZ in either CA1 or DG.

Discussion

The primary goal of these studies was to determine the effects of genetic loss of DBI on synaptic inhibition in the murine hippocampus. Our data show that the loss of DBI results in an enhancement of inhibition in CA1 pyramidal cells, as demonstrated in increased mIPSC frequency and amplitude. Surprisingly, we found that the loss of DBI leads to decreased mIPSC amplitude in DG granule cells, providing novel evidence of a diametric modulation of inhibition by DBI within the hippocampus. Additionally, we determined that the changes in mIPSC frequency in CA1 pyramidal cells in $DBI^{-/-}$ mice are not due to alterations in vesicular release probability, suggesting that the loss of DBI may alter the number of synaptic contacts onto principal cells. We also found that loss of DBI did not impact the responsiveness of either CA1 pyramidal and DG granule cells to DZP or FLZ application. These results provide evidence that DBI is capable of bidirectionally modulating GABAergic transmission in the hippocampus, and support the conclusion that DBI-mediated modulation of inhibition is distinctly localized in specific subregions of brain structures.

DBI appears to be a complex and multifunctional peptide, with both positive and negative allosteric modulatory effects on $GABA_A$Rs reported. Surprisingly, the present results provide support for both conclusions within the hippocampus, with a loss of DBI leading to an enhancement of inhibition in CA1 and an attenuation of inhibition in DG. Furthermore, these data indicate that the loss of DBI leads to both pre- and postsynaptic alterations of GABAergic transmission in the hippocampus. Although the mechanisms behind this diametric modulation remain elusive, some potential hypotheses have emerged. $GABA_A$Rs are pentameric hetero-oligomers in which subunit combinations are assembled from a set of

19 subunit possibilities (Olsen and Sieghart, 2008), leading to a large diversity of subunit compositions. Subunit composition directly influences the biophysical properties of $GABA_A$Rs, including the single-channel conductance and responsiveness to allosteric modulators (Hevers and Luddens, 1998; Mody and Pearce, 2004). Therefore, it is plausible that DBI may exert its influence on different postsynaptic $GABA_A$R subtypes in CA1 versus DG (Hörtnagl et al., 2013), and/or that the loss of DBI may lead to compensatory modifications in $GABA_A$R subunit composition in each subregion. Another possibility is that DBI may be cleaved differently in CA1 compared to DG, and thus distinct DBI processing products may be produced in these regions. The manner in which the DBI peptide is endogenously cleaved has not been determined, and the enzymes responsible for cleavage are also unknown. Future experiments could utilize targeted analytical chemistry techniques such as mass spectrometry to investigate the presence of specific DBI cleavage products in each hippocampal subregion.

We originally hypothesized that cells from $DBI^{-/-}$ mice would be more sensitive to DZP due to a lack of competition at the BZ-binding site. However, we observed that CA1 and DG cells from both $DBI^{+/+}$ and $DBI^{-/-}$ mice responded equally to DZP. One potential explanation for this result may be that the concentration of DZP was too robust, such that it saturated GABAergic synapses and masked a subtler effect. DZP may act via two separate mechanisms that depend on the concentration applied: a nanomolar component that depends on the γ2 subunit; and a micromolar component that does not require the γ2 subunit (Walters et al., 2000). We also found that responses to FLZ were not altered in mice genetically lacking DBI signaling, and that the administration of FLZ did not affect mIPSC properties of CA1 pyramidal cells from either genotype. However, we did observe an increase in mIPSC amplitude with both low- and high-dose FLZ application in DG granule cells from both $DBI^{+/+}$ and $DBI^{-/-}$ mice. FLZ is a weak positive allosteric modulator of $GABA_A$Rs containing certain subunit combinations, specifically combinations including the α2, α3, or α4 subunits (Ramerstorfer et al., 2010). α3 subunit-containing receptors are rarely expressed in DG (Sperk et al., 1997). Therefore, these effects may be mediated by synapses expressing α2 or α4 subunit-containing receptors. However, α4 subunit-containing receptors are insensitive to BZs (Chandra et al., 2006), thus raising the likelihood that the FLZ-induced increase in mIPSC amplitude is mediated by α2-containing receptors. This effect was only seen in DG, providing further support for future investigations into the subunit combinations of $GABA_A$Rs in CA1 versus DG. The lack of differences seen between genotypes after pharmacological BZ-binding site manipulations of $GABA_A$Rs suggests that the DBI-dependent modulation of inhibition in these regions is likely not endozepine-related. Rather, the observed changes in synaptic inhibition in the $DBI^{-/-}$ mouse hippocampus may reflect other mechanisms, such as an alteration of a critical metabolic pathway or a DBI-dependent modification in neuronal development.

Although DBI is primarily recognized as acting at the BZ-binding site to modulate $GABA_A$Rs, DBI may also indirectly modulate inhibitory transmission via the mitochondrial benzodiazepine receptor, also known as translocator protein (TSPO) (Papadopoulos et al., 1991). The binding of DBI to TSPO has been demonstrated to stimulate neurosteroid biosynthesis (Korneyev et al., 1993). Neurosteroids are potent modulators of $GABA_A$Rs (Belelli and Lambert, 2005), and both positive and negative allosteric modulation of

$GABA_A$Rs by neurosteroids have been demonstrated (Wang, 2011). Therefore, it is possible that the effects seen in both hippocampal subregions after the genetic loss of DBI may be due to changes in the activity of TSPO, leading to alterations in neurosteroidogenesis and subsequent modulation of inhibition in the hippocampus. The lack of differences between $DBI^{+/+}$ and $DBI^{-/-}$ mice in response to applications of a BZ-site agonist (DZP) and antagonist (FLZ) supports the possibility of an indirect neurosteroid-mediated modulation of $GABA_A$Rs by DBI. Further investigations of the subunit composition of $GABA_A$Rs in these regions and subunit-associated differences in DBI sensitivity may provide insight into these possibilities.

Recent evidence supports a role for DBI in the regulation of neurogenesis. In the subgranular zone (SGZ), the region that produces granule cells in DG, DBI appears to critically regulate the balance between preserving the neural stem cell pool and the development of new granule cells. Specifically, genetic knockdown of DBI led to fewer neural stem cells and a shift towards mature granule cell development, while a genetic overexpression of DBI led to a greater neural stem cell population and a reduction in neurogenesis (Dumitru et al., 2017). Our experiments were performed on constitutive DBI $^{-/-}$ mice, in which exon 2 of the *Dbi* gene is deleted throughout the lifespan. Therefore, it is possible that the development of hippocampal neurons is fundamentally altered to compensate for the lack of DBI signaling. In addition, other developmental compensations may arise in $DBI^{-/-}$ mice, as the *Dbi* gene appears to serve multiple cellular functions, including general housekeeping duties (Mandrup et al., 1992). Future studies could make use of more advanced transgenic technology to overcome these issues, such as utilizing an inducible DBI knockout mouse, a nervous system-specific transgenic mouse line, or using Cre-dependent viral vectors for region-specific deletions.

In summary, the present results demonstrate that the genetic deletion of DBI signaling diametrically alters synaptic inhibition in the murine hippocampus in a subregion-specific manner. $DBI^{-/-}$ mice demonstrated an enhancement of inhibition in CA1 pyramidal cells, but displayed an attenuation of inhibition in DG granule cells. Presynaptic release probability remained constant in both genotypes, and $DBI^{-/-}$ mice did not differ from DBI^{+r} + mice in their response to BZ-binding site agonism or antagonism. These results lay the groundwork for future investigations into the role of DBI in the modulation of synaptic inhibition in the hippocampus.

Acknowledgements

We thank Dr. Susanne Mandrup for the gift of founder mice for our DBI knockout colony and Amin Ghane, Steven Rhoads, and Ammar Ujjainwala for assistance with mouse colony maintenance and genotyping. This work was supported by the Brain and Behavior Research Foundation (NARSAD Young Investigator Grant 24086, C.A.C.) and start-up funds from the University of Illinois at Urbana-Champaign (C.A.C.). C.A.C is also supported by National Institute of Neurological Disorders and Stroke R01 NS105825. C.A.C. designed the experiments; C.D.C. performed experiments, analyzed data, and prepared the figures; C.D.C. and C.A.C. wrote the manuscript.

Abbreviations:

BZ	benzodiazepine
DBI	diazepam binding inhibitor

DG	dentate gyrus
DZP	diazepam
eIPSC	evoked inhibitory postsynaptic current
FLZ	flumazenil
GABA	γ-aminobutyric acid
$GABA_AR$	$GABA_A$ receptor
mIPSC	miniature inhibitory postsynaptic current
ODN	octadecaneuropeptide
PPR	paired-pulse ratio

References

Alfonso J, Le Magueresse C, Zuccotti A, Khodosevich K, Monyer H (2012) Diazepam binding inhibitor promotes progenitor proliferation in the postnatal SVZ by reducing GABA signaling. Cell Stem Cell 10:76–87. [PubMed: 22226357]

Alho H, Bovolin P, Jenkins D, Guidotti A, Costa E (1989) Cellular and subcellular localization of an octadecaneuropeptide derived from diazepam binding inhibitor: immunohistochemical studies in the rat brain. J Chem Neuroanat 2:301–318. [PubMed: 2482048]

Alho H, Harjuntausta T, Schultz R, Pelto-Huikko M, Bovolin P (1991) Immunohistochemistry of diazepam binding inhibitor (DBI) in the central nervous system and peripheral organs: its possible role as an endogenous regulator of different types of benzodiazepine receptors. Neuropharmacology 30:1381–1386. [PubMed: 1664066]

Alho H, Costa E, Ferrero P, Fujimoto M, Cosenza-Murphy D, Guidotti A (1985) Diazepambinding inhibitor: a neuropeptide located in selected neuronal populations of rat brain. Science 229:179–182. [PubMed: 3892688]

Ball JA, Ghatei MA, Sekiya K, Krausz T, Bloom SR (1989) Diazepam binding inhibitor-like immunoreactivity (51–70): distribution in human brain, spinal cord and peripheral tissues. Brain Res 479:300–305. [PubMed: 2924161]

Belelli D, Lambert JJ (2005) Neurosteroids: endogenous regulators of the GABAA receptor. Nat Rev Neurosci 6:565–575. [PubMed: 15959466]

Bianchi MT (2010) Context dependent benzodiazepine modulation of GABAA receptor opening frequency. Curr Neuropharmacol 8:10–17. [PubMed: 20808542]

Bormann J (1991) Electrophysiological characterization of diazepam binding inhibitor (DBI) on GABAA receptors. Neuropharmacology 30:1387–1389. [PubMed: 1723508]

Braestrup C, Squires RF (1977) Specific benzodiazepine receptors in rat brain characterized by high-affinity (3H) diazepam binding. Proc Natl Acad Sci USA 74:3805–3809. [PubMed: 20632]

Chandra D, Jia F, Liang J, Peng Z, Suryanarayanan A, Werner D, Spigelman I, Houser C, Olsen R, Harrison N (2006) GABAA receptor α4 subunits mediate extrasynaptic inhibition in thalamus and dentate gyrus and the action of gaboxadol. Proc Natl Acad Sci USA 103:15230–15235. [PubMed: 17005728]

Christian CA, Huguenard JR (2013) Astrocytes potentiate GABAergic transmission in the thalamic reticular nucleus via endozepine signaling. Proc Natl Acad Sci USA 110:20278–20283. [PubMed: 24262146]

Christian CA, Herbert AG, Holt RL, Peng K, Sherwood KD, Pangratz-Fuehrer S, Rudolph U, Huguenard JR (2013) Endogenous positive allosteric modulation of GABA(A) receptors by diazepam binding inhibitor. Neuron 78:1063–1074. [PubMed: 23727119]

Costa E, Guidotti A (1985) Endogenous ligands for benzodiazepine recognition sites. Biochem Pharmacol 34:3399–3403. [PubMed: 2413860]

Costa E, Guidotti A (1991) Diazepam binding inhibitor (DBI): a peptide with multiple biological actions. Life Sci 49:325–344. [PubMed: 1649940]

Dobrunz LE, Stevens CF (1997) Heterogeneity of release probability, facilitation, and depletion at central synapses. Neuron 18:995–1008. [PubMed: 9208866]

Dumitru I, Neitz A, Alfonso J, Monyer H (2017) Diazepam Binding Inhibitor Promotes Stem Cell Expansion Controlling Environment-Dependent Neurogenesis. Neuron 94:125–137. [PubMed: 28343864]

Farzampour Z, Reimer RJ, Huguenard J (2015) Chapter Five-Endozepines. Adv Pharmacol 72:147–164. [PubMed: 25600369]

Ferrarese C, Appollonio I, Frigo M, Piolti R, Tamma F, Frattola L (1989) Distribution of a putative endogenous modulator of the GABA ergic system in human brain. Neurology 39:443–445. [PubMed: 2927661]

Ferrero P, Santi M, Conti-Tronconi B, Costa E, Guidotti A (1986) Study of an octadecaneuropeptide derived from diazepam binding inhibitor (DBI): biological activity and presence in rat brain. Proc Natl Acad Sci USA 83:827–831. [PubMed: 3456171]

Guidotti A, Forchetti CM, Corda MG, Konkel D, Bennett CD, Costa E (1983) Isolation, characterization, and purification to homogeneity of an endogenous polypeptide with agonistic action on benzodiazepine receptors. Proc Natl Acad Sci USA 80:3531–3535. [PubMed: 6304714]

Hevers W, Luddens H (1998) The diversity of GABAA receptors. Mol Neurobiol 18:35–86. [PubMed: 9824848]

Hörtnagl H, Tasan R, Wieselthaler A, Kirchmair E, Sieghart W, Sperk G (2013) Patterns of mRNA and protein expression for 12 GABAA receptor subunits in the mouse brain. Neuroscience 236:345–372. [PubMed: 23337532]

Hunkeler W, Mohler H, Pieri L, Polc P, Bonetti EP, Cumin R, Schaffner R, and Haefely W (1981) Selective antagonists of benzodiazepines. Nature, 290:514–516. [PubMed: 6261143]

Iversen L (1977) Anti-anxiety receptors in the brain? Nature 266:678.

Kim J, Alger BE (2001) Random response fluctuations lead to spurious paired-pulse facilitation. J Neurosci 21:9608–9618. [PubMed: 11739571]

King G, Knox J, Dingledine R (1985) Reduction of inhibition by a benzodiazepine antagonist, Ro15–1788, in the rat hippocampal slice. Neuroscience 15:371–378. [PubMed: 2991811]

Korneyev A, Pan B, Polo A, Romeo E, Guidotti A, Costa E (1993) Stimulation of brain pregnenolone synthesis by mitochondrial diazepam binding inhibitor receptor ligands in vivo. J Neurochem 61:1515–1524. [PubMed: 8397297]

Leroy C, Poisbeau P, Keller A, Nehlig A (2004) Pharmacological plasticity of GABAA receptors at dentate gyrus synapses in a rat model of temporal lobe epilepsy. J Physiol 557:473–487. [PubMed: 15034126]

Liu X, Li Y, Zhou L, Chen H, Su Z, Hao W (2005) Conditioned place preference associates with the mRNA expression of diazepam binding inhibitor in brain regions of the addicted rat during withdrawal. Brain Res Mol Brain Res 137:47–54. [PubMed: 15950760]

Malagon M, Vaudry H, Van Strien F, Pelletier G, Gracia-Navarro F, Tonon M (1993) Ontogeny of diazepam-binding inhibitor-related peptides (endozepines) in the rat brain. Neuroscience 57:777–786. [PubMed: 8309536]

Mandrup S, Hummel R, Ravn S, Jensen G, Andreasen PH, Gregersen N, Knudsen J, Kristiansen K (1992) Acyl-CoA-binding protein/diazepam-binding inhibitor gene and pseudogenes: a typical housekeeping gene family. J Mol Biol 228:1011–1022. [PubMed: 1469708]

Mody I, Pearce RA (2004) Diversity of inhibitory neurotransmission through GABA A receptors. Trends Neurosci 27:569–575. [PubMed: 15331240]

Möhler H (2014) Endogenous Benzodiazepine Site Peptide Ligands Operating Bidirectionally In Vivo in Neurogenesis and Thalamic Oscillations. Neurochem Res 39:1032–1036. [PubMed: 24715673]

Möhler H, Okada T (1977) Properties of 3H-diazepam binding to benzodiazepine receptors in rat cerebral cortex. Life Sci 20:2101–2110. [PubMed: 18642]

Neess D, Bek S, Engelsby H, Gallego SF, F^rgeman NJ (2015) Long-chain acyl-CoA esters in metabolism and signaling: role of acyl-CoA binding proteins. Prog Lipid Res 59:1–25. [PubMed: 25898985]

Neess D, Bloksgaard M, Bek S, Marcher AB, Elle IC, Helledie T, Due M, Pagmantidis V, Finsen B, Wilbertz J, Kruhoffer M, Faergemen N, Mandrup S (2011) Disruption of the acyl-CoA-binding protein gene delays hepatic adaptation to metabolic changes at weaning. J Biol Chem 286:3460–3472. [PubMed: 21106527]

Olmos-Serrano JL, Paluszkiewicz SM, Martin BS, Kaufmann WE, Corbin JG, Huntsman MM (2010) Defective GABAergic neurotransmission and pharmacological rescue of neuronal hyperexcitability in the amygdala in a mouse model of fragile X syndrome. J Neurosci 30:9929–9938. [PubMed: 20660275]

Olsen RW, Sieghart W (2008) International Union of Pharmacology. LXX. Subtypes of γ-aminobutyric acidA receptors: classification on the basis of subunit composition, pharmacology, and function. Update. Pharmacol Rev 60:243–260. [PubMed: 18790874]

Papadopoulos V, Berkovich A, Krueger K, Costa E, Guidotti A (1991) Diazepam binding inhibitor and its processing products stimulate mitochondrial steroid biosynthesis via an interaction with mitochondrial benzodiazepine receptors. Endocrinology 129:1481–1488. [PubMed: 1651852]

Ramerstorfer J, Furtmuller R, Vogel E, Huck S, Sieghart W (2010) The point mutation γ2F771 changes the potency and efficacy of benzodiazepine site ligands in different GABA A receptor subtypes. Eur J Pharmacol 636:18–27. [PubMed: 20303942]

Sherrin T, Blank T, Saravana R, Rayner M, Spiess J, Todorovic C (2009) Region specific gene expression profile in mouse brain after chronic corticotropin releasing factor receptor 1 activation: the novel role for diazepam binding inhibitor in contextual fear conditioning. Neuroscience 162:14–22. [PubMed: 19362130]

Sieghart W (2015) Chapter Three-Allosteric Modulation of GABA A Receptors via Multiple Drug-Binding Sites. Adv Pharmacol 72:53–96. [PubMed: 25600367]

Siiskonen H, Oikari S, Korhonen V-P, Pitkanen A, Voikar V, Kettunen M, Hakumaki J, Wahlfors T, Pussinen R, Penttonen M, Kiehne K, Kaasinen SK, Alhonen L, Janne J, Herzig KH (2007) Diazepam binding inhibitor overexpression in mice causes hydrocephalus, decreases plasticity in excitatory synapses and impairs hippocampus-dependent learning. Mol Cell Neurosci 34:199–208. [PubMed: 17150371]

Sperk G, Schwarzer C, Tsunashima K, Fuchs K, Sieghart W (1997) GABA A receptor subunits in the rat hippocampus I: immunocytochemical distribution of 13 subunits. Neuroscience 80:987–1000. [PubMed: 9284055]

Thomson AM (2000) Facilitation, augmentation and potentiation at central synapses. Trends Neurosci 23:305–312. [PubMed: 10856940]

Twyman RE, Rogers CJ, Macdonald RL (1989) Differential regulation of γ-aminobutyric acid receptor channels by diazepam and phenobarbital. Ann Neurol 25:213–220. [PubMed: 2471436]

Ujjainwala AL, Courtney CD, Rhoads SG, Rhodes JS, Christian CA (2018) Genetic loss of diazepam binding inhibitor in mice impairs social interest. Genes Brain Behav e:12442.

Vicini S, Alho H, Costa E, Mienville J, Santi M, Vaccarino F (1986) Modulation of gamma-aminobutyric acid-mediated inhibitory synaptic currents in dissociated cortical cell cultures. Proc Natl Acad Sci USA 83:9269–9273. [PubMed: 3097650]

Vidnyánszky Z, Gorcs TJ, Hamori J (1994) Diazepam binding inhibitor fragment 33–50 (octadecaneuropeptide) immunoreactivity in the cerebellar cortex is restricted to glial cells. Glia 10:132–141. [PubMed: 8168866]

Walters RJ, Hadley SH, Morris KD, Amin J (2000) Benzodiazepines act on GABAA receptors via two distinct and separable mechanisms. Nat Neurosci 3:1274–1281. [PubMed: 11100148]

Wang M (2011) Neurosteroids and GABA-A receptor function. Front Endocrinol (Lausanne) 2:44. [PubMed: 22654809]

Xu J-Y, Sastry B (2005) Benzodiazepine involvement in LTP of the GABA-ergic IPSC in rat hippocampal CA1 neurons. Brain Res 1062:134–143. [PubMed: 16266690]

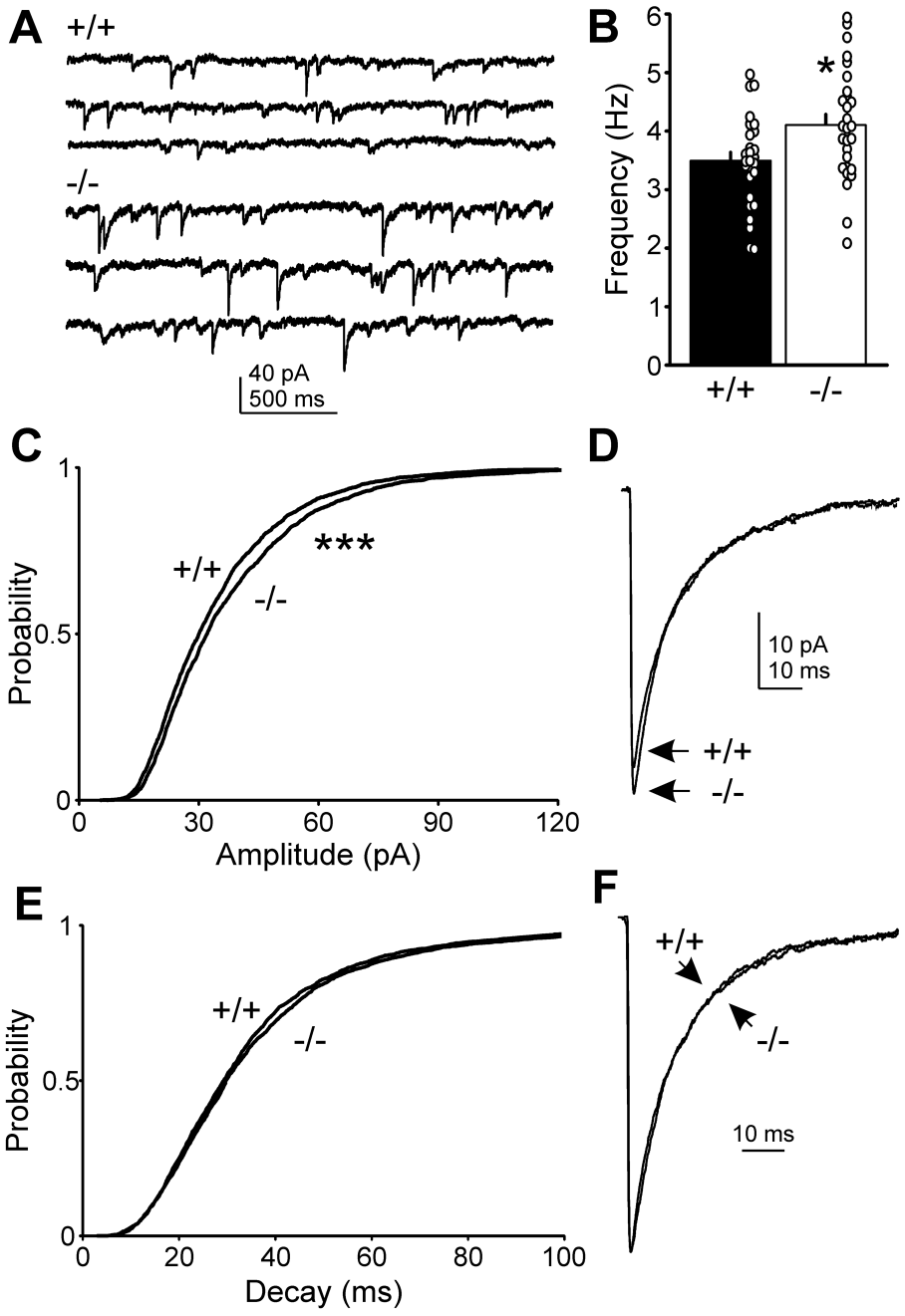

Figure 1: Genetic loss of DBI increases mIPSC amplitude and frequency in CA1 pyramidal cells.

(A) Representative mIPSC traces recorded from individual pyramidal cells from $DBI^{+/+}$ (top traces) and $DBI^{-/-}$ mice (bottom traces). (B) Mean + SEM of mIPSC frequency in CA1 pyramidal cells from $DBI^{+/+}$ (black bar, n=28 cells from 11 mice) and $DBI^{-/-}$ mice (white bar, n=27 cells from 10 mice) (*p<0.05, Student's t-test). Open circles represent values from individual cells. (C) Cumulative probability distributions comparing mIPSC amplitude in $DBI^{+/+}$ (n=2800 events from 28 cells from 11 mice) and $DBI^{-/-}$ mice (n=2700 events from 27 cells from 10 mice) (***p<0.001, KS test). (D) Averaged mIPSC traces from

representative $DBI^{+/+}$ and $DBI^{-/-}$ cells. (E) Cumulative probability distributions comparing mIPSC decay in CA1 pyramidal cells from $DBI^{+/+}$ (n=2800 events from 28 cells from 11 mice) and $DBI^{-/-}$ mice (n=2700 events from 27 cells from 10 mice). (F) Averaged mIPSC traces from representative $DBI^{+/+}$ and $DBI^{-/-}$ cells, normalized to peak amplitude.

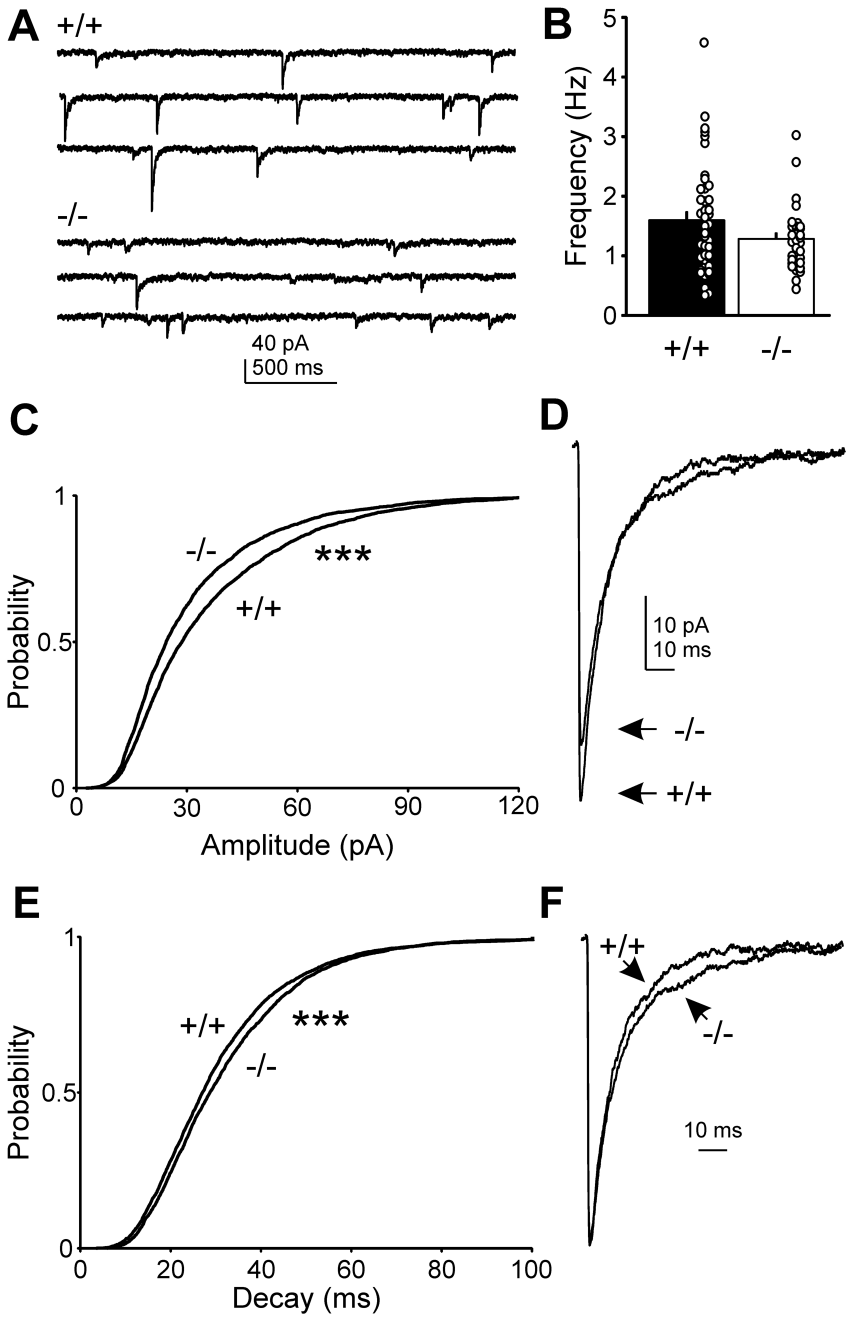

Figure 2: Genetic loss of DBI decreases mIPSC amplitude in DG granule cells, but increases mIPSC decay.

(A) Representative mIPSC traces recorded from individual granule cells from $DBI^{+/+}$ (top traces) and $DBI^{-/-}$ mice (bottom traces). (B) Mean + SEM of mIPSC frequency in DG granule cells from $DBI^{+/+}$ (black bars, n=43 cells from 15 mice) and $DBI^{-/-}$ mice (white bars, n=31 cells from 10 mice). Open circles represent values from individual cells. (C) Cumulative probability distributions comparing mIPSC amplitude in $DBI^{+/+}$ (n=4025 events from 43 cells from mice) and $DBI^{-/-}$ mice (n=2929 events from 31 cells from 10 mice) (***p<0.001, KS test). (D) Averaged mIPSC traces from representative $DBI^{+/+}$ and $DBI^{-/-}$

granule cells. (E) Cumulative probability distributions comparing mIPSC decay in DG granule cells from $DBI^{+/+}$ (n=4025 events from 43 cells from 15 mice) and $DBI^{-/-}$ mice (n=2929 events from 31 cells from 10 mice) (***p<0.001, KS test). (F) Averaged mIPSC traces from representative $DBI^{+/+}$ and $DBI^{-/-}$ granule cells, normalized to peak amplitude.

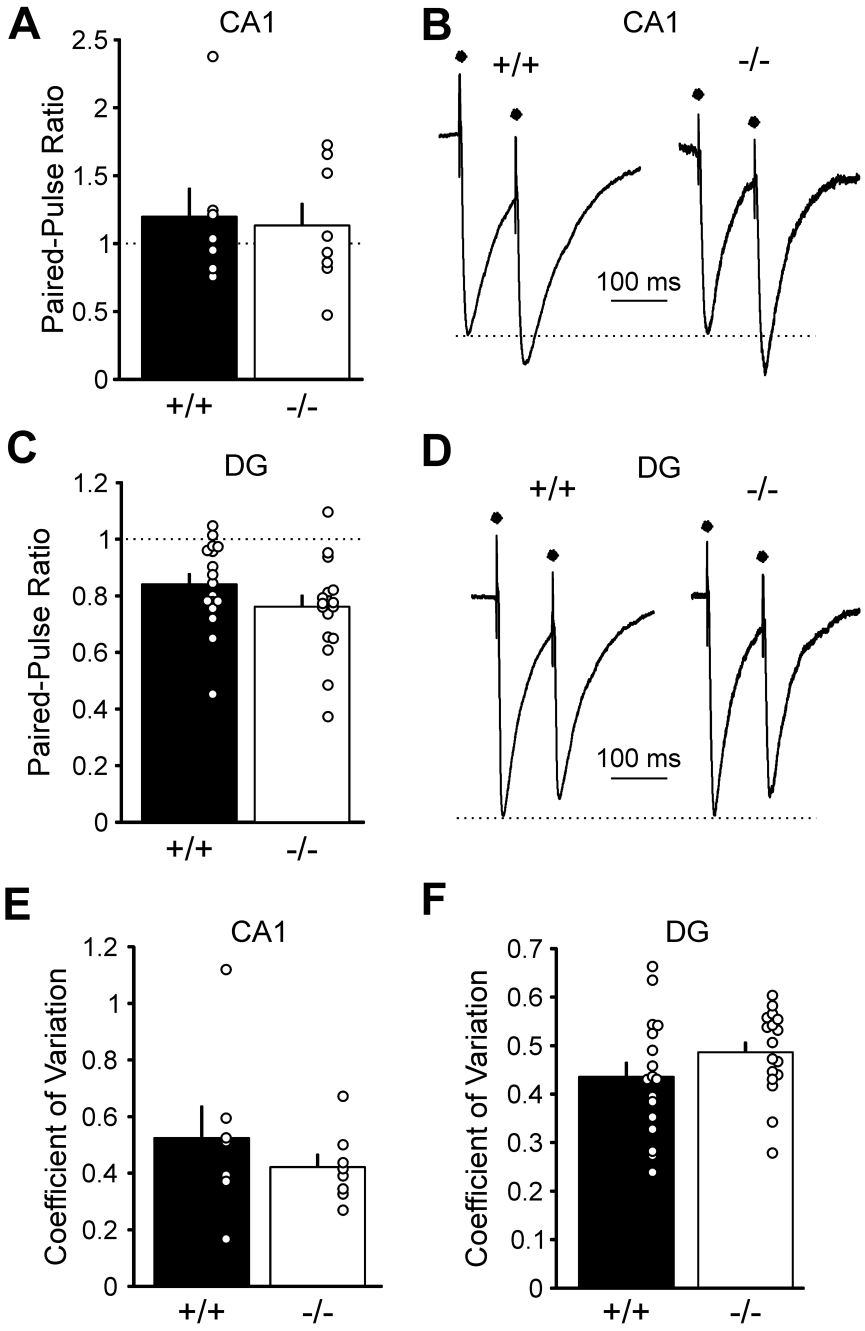

Figure 3: No differences between DBI$^{+/+}$ and DBI$^{-/-}$ mice in paired-pulse ratio of evoked IPSCs.

(A) Mean + SEM of PPR from eIPSCs in CA1 pyramidal cells from DBI$^{+/+}$ (black bar, n=8 cells from 7 mice) and DBI$^{-/-}$ mice (white bar, n=8 cells from 5 mice). Open circles represent values from individual cells. (B) Averaged PPR traces from representative DBI$^{+/+}$ (left) and DBI$^{-/-}$ (right) pyramidal cells, normalized to peak amplitude of the first response. Black dots indicate times of electrical stimulus application; stimulus artifacts are truncated for clarity. (C) Mean + SEM of PPR from eIPSCs in DG granule cells from DBI$^{+/+}$ (black bar, n=17 cells from 8 mice) and DBI$^{-/-}$ mice (white bar, n=18 cells from 8 mice). Open

circles represent values from individual cells. (D) Averaged PPR traces from representative $DBI^{+/+}$ (left) and $DBI^{-/-}$ (right) granule cells, normalized to peak amplitude of the first response. Black dots indicate times of electrical stimulus application; stimulus artifacts are truncated for clarity. (E-F) Mean + SEM of the coefficient of variation of eIPSCs in CA1 pyramidal cells (E) and DG granule cells (F) from $DBI^{+/+}$ (black bars, n=17 cells from 8 mice) and $DBI^{-/-}$ mice (white bars, n=18 cells from 8 mice). Open circles represent values from individual cells.

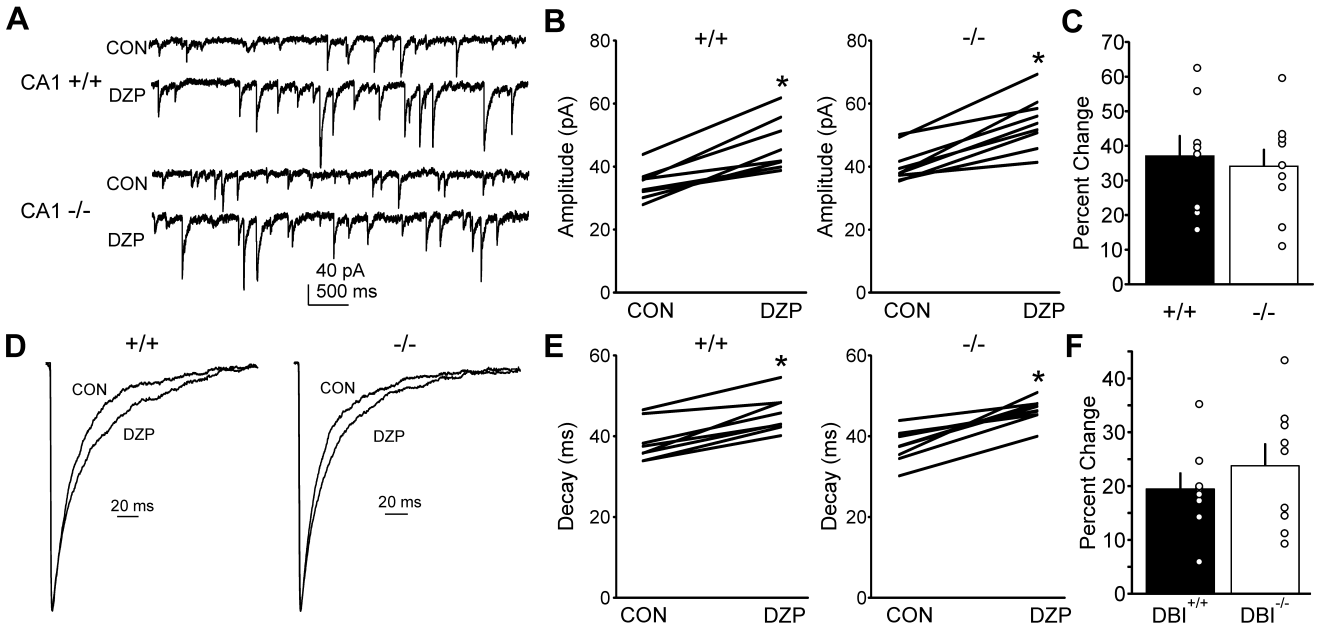

Figure 4: No differences between genotypes in mIPSC amplitude or decay after diazepam application in CA1 pyramidal cells.

(A) Representative mIPSC traces from individual CA1 pyramidal cells before (CON) and during DZP treatment from $DBI^{+/+}$ (top) and $DBI^{-/-}$ (bottom) mice. (B) mIPSC amplitude in individual CA1 pyramidal cells from $DBI^{+/+}$ (left, n=8 cells from 4 mice) and $DBI^{-/-}$ mice (right, n=9 cells from 5 mice) before (CON) and during DZP treatment (*p<0.05, paired t-test). (C) Mean + SEM of the percentage change in mIPSC amplitude after diazepam application in CA1 pyramidal cells from $DBI^{+/+}$ (black bar) and $DBI^{-/-}$ mice (white bar). Open circles represent values from individual cells. (D) Averaged mIPSC traces from representative CA1 pyramidal cells before (CON) and during DZP treatment, normalized to peak amplitude, from $DBI^{+/+}$ (left) and $DBI^{-/-}$ mice (right). (E) mIPSC decay in individual CA1 pyramidal cells from $DBI^{+/+}$ (left) and $DBI^{-/-}$ mice (right) before (CON) and during DZP treatment (*p<0.05, paired t-test). (F) Mean + SEM of the percentage change in mIPSC decay after DZP application in CA1 pyramidal cells from $DBI^{+/+}$ (black bar) and $DBI^{-/-}$ mice (white bar). Open circles represent values from individual cells.

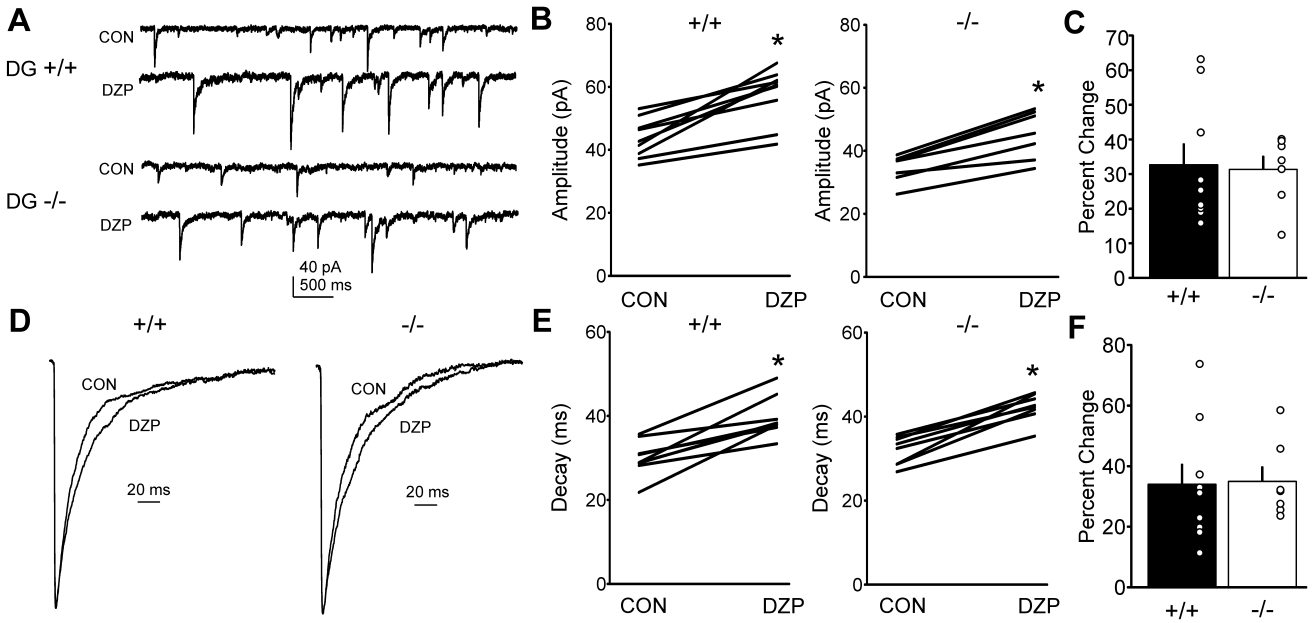

Figure 5: No differences between genotypes in mIPSC amplitude or decay after diazepam application in DG granule cells.

(A) Representative mIPSC traces from individual DG granule cells before (CON) and during DZP treatment from $DBI^{+/+}$ (top) and $DBI^{-/-}$ mice (bottom). (B) mIPSC amplitude in individual DG granule cells from $DBI^{+/+}$ (left, n=9 cells from 3 mice) and $DBI^{-/-}$ mice (right, n=7 cells from 2 mice) before (CON) and during DZP treatment (*p<0.05, paired t-test). (C) Mean + SEM of the percentage change in mIPSC amplitude after DZP application in DG granule cells from $DBI^{+/+}$ (black bar) and $DBI^{-/-}$ mice (white bar). Open circles represent values from individual cells. (D) Averaged mIPSC traces from representative DG granule cells before (CON) and during DZP treatment, normalized to peak amplitude, from $DBI^{+/+}$ (left) and $DBI^{-/-}$ mice (right). (E) mIPSC decay in individual DG granule cells from $DBI^{+/+}$ (left) and $DBI^{-/-}$ mice (right) before (CON) and during DZP treatment (*p<0.05, paired t-test). (F) Mean + SEM of the percentage change in mIPSC decay after DZP application in DG granule cells from $DBI^{+/+}$ (black bar) and $DBI^{-/-}$ mice (white bar). Open circles represent values from individual cells.

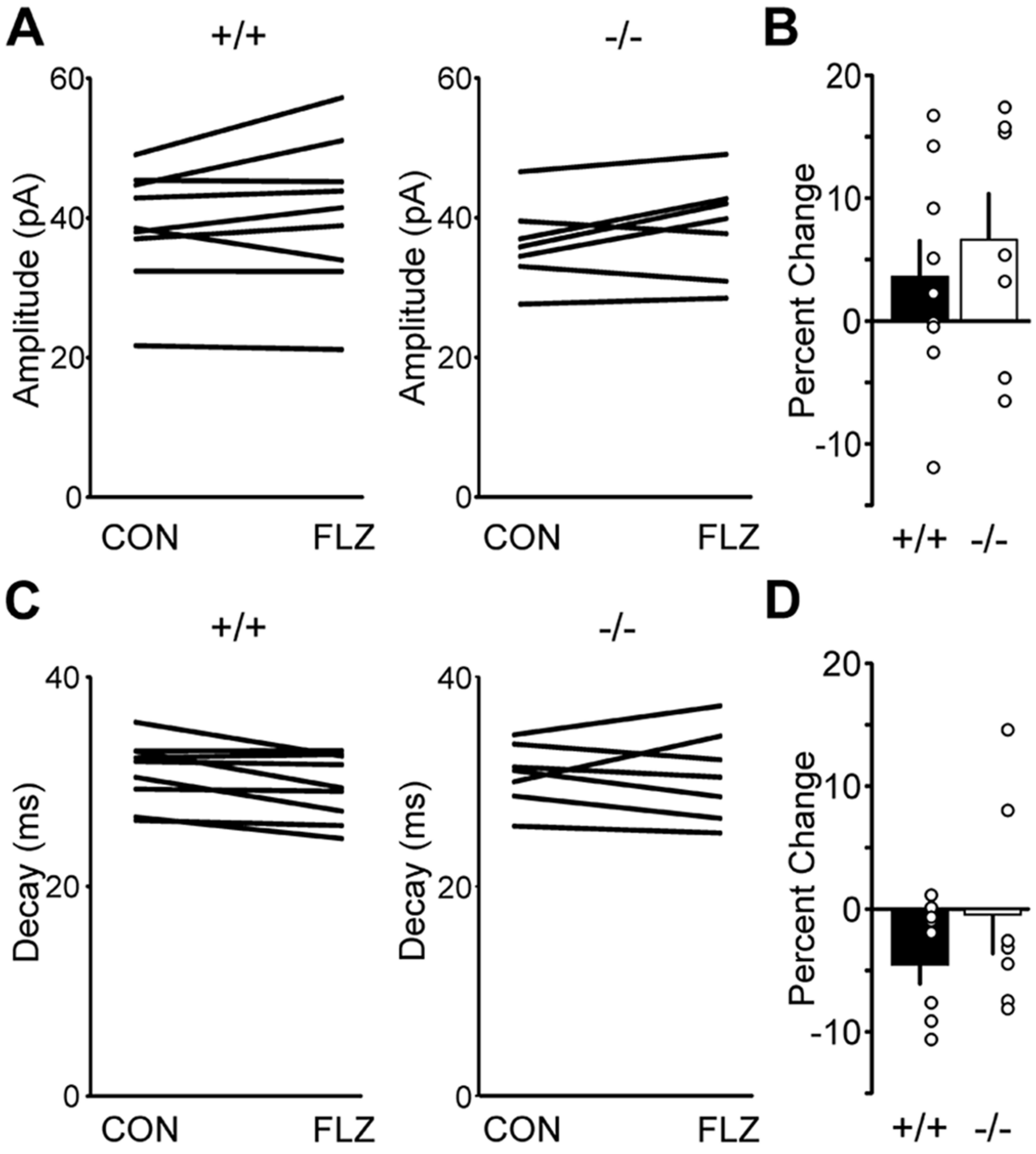

Figure 6: 1 μM flumazenil does not change mIPSC amplitude or decay in CA1 pyramidal cells from either genotype.

(A) mIPSC amplitude in individual CA1 pyramidal cells from $DBI^{+/+}$ (left, n=9 cells from 5 mice) and $DBI^{-/-}$ mice (right, n=7 cells from 3 mice) before (CON) and during 1 μM FLZ treatment. (B) Mean + SEM of the percentage change in mIPSC amplitude after FLZ application in CA1 pyramidal cells from $DBI^{+/+}$ (black bar) and $DBI^{-/-}$ mice (white bar). Open circles represent values from individual cells. (C) mIPSC decay in individual CA1 pyramidal cells from $DBI^{+/+}$ (left) and $DBI^{-/-}$ mice (right) before (CON) and during FLZ treatment. (D) Mean + SEM of the percentage change in mIPSC decay after FLZ application

in CA1 pyramidal cells from $DBI^{+/+}$ (black bar) and $DBI^{-/-}$ mice (white bar). Open circles represent values from individual cells.

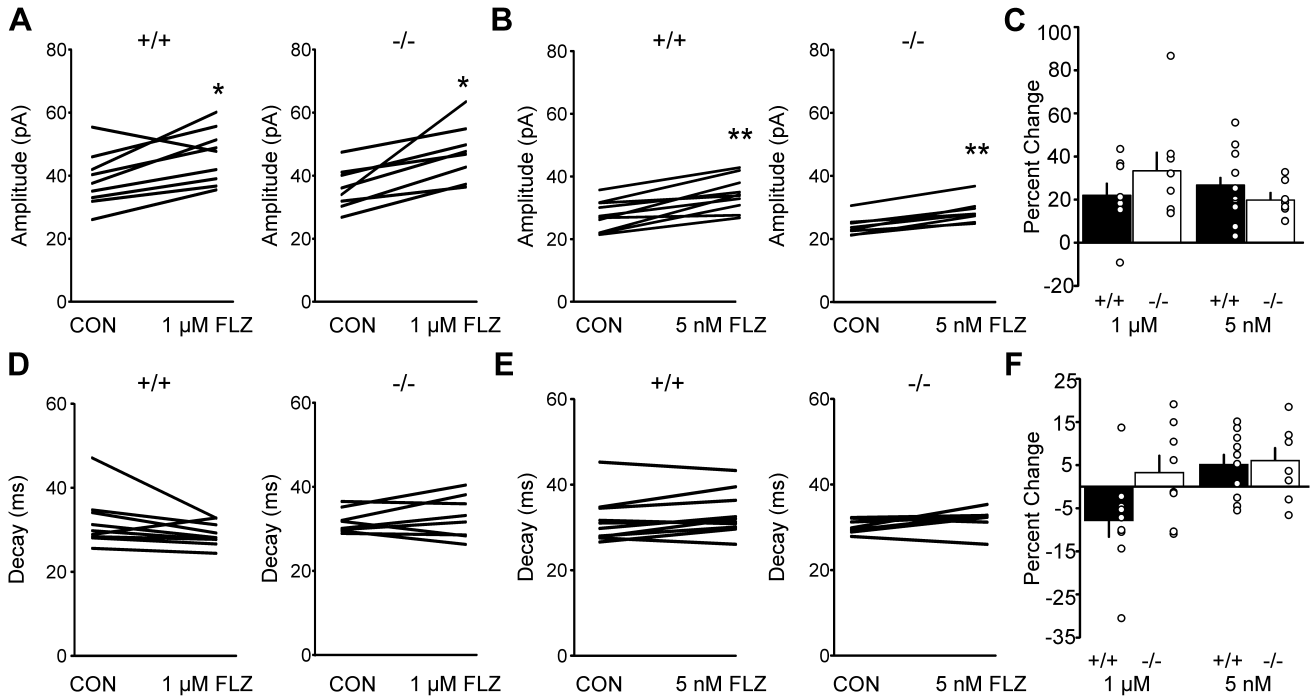

Figure 7: Both 5 nM and 1 μM flumazenil increase mIPSC amplitude in DG granule cells with no effect on decay.

(A) mIPSC amplitude in individual DG granule cells from $DBI^{+/+}$ (left, n=9 cells from 4 mice) and $DBI^{-/-}$ mice (right, n=8 cells from 3 mice) before (CON) and during 1 μM FLZ treatment (*p<0.05, paired t-test). (B) mIPSC amplitude in individual DG granule cells from $DBI^{+/+}$ (left, n=10 cells from 4 mice) and $DBI^{-/-}$ mice (right, n=9 cells from 3 mice) before (CON) and during 5 nM FLZ treatment (**p<0.01). (C) Mean + SEM of the percentage change in mIPSC amplitude after either 1 μM or 5 nM FLZ application in DG granule cells from $DBI^{+/+}$ (black bars) and $DBI^{-/-}$ mice (white bars). Open circles represent values from individual cells. (D) mIPSC decay in individual DG granule cells from $DBI^{+/+}$ (left, n=9 cells from 4 mice) and $DBI^{-/-}$ mice (right, 8 cells from 3 mice) before (CON) and during 1 μM FLZ treatment. (E) mIPSC decay in individual DG granule cells from $DBI^{+/+}$ (left, n=10 cells from 4 mice) and $DBI^{-/-}$ mice (right, n=9 cells from 3 mice) before (CON) and during 5 nM FLZ treatment. (F) Mean + SEM of the percentage change in mIPSC decay after either 1 μM or 5 nM FLZ application in DG granule cells in $DBI^{+/+}$ (black bars) and $DBI^{-/-}$ mice (white bars). Open circles represent values from individual cells.

Table 1:

mIPSC amplitude and decay in CA1 pyramidal cells and DG granule cells, incorporating all unitary events collected.

Mean ± SEM for mIPSC amplitude (pA) and decay (ms).

	CA1		DG	
	DBI$^{+/+}$	**DBI$^{-/-}$**	**DBI$^{+/+}$**	**DBI$^{-/-}$**
Amplitude	35.55 ± 1.20	38.57 ± 1.13$^{\$}$	37.19 ± 1.21	31.73 ± 1.23**
Decay	34.90 ± 1.01	34.93 ± 0.85	30.80 ± 1.12	34.43 ± 1.02*

** $p<0.01$

* $p<0.05$

$^{\$}$ $p=0.07$

Student's t-test